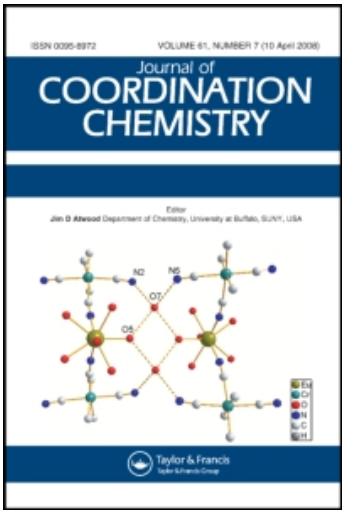

Journal of Coordination Chemistry
Publication details, including instructions for authors and subscription information:
http://www.informaworld.com/smpp/title~content=t713455674

THE NATURE OF METAL-AZIDE INTERACTIONS IN A HIGH-VALENT TETRAAZIDO-MANGANESE(IV) COMPLEX. ISOLATION, STRUCTURE AND PROPERTIES, INCLUDING UV-*VIS*, EPR AND RESONANCE RAMAN SPECTROSCOPY OF [Mn(bpy)(N_3)$_4$] (bpy = 2,2'-bipyridine)

Bakul C. Dave[a]; Roman S. Czernuszewicz[b]
[a] Department of Chemistry and Biochemistry, University of California at Los Angeles, Los Angeles, CA [b] Department of Chemistry, University of Houston, Houston, TX

To cite this Article Dave, Bakul C. and Czernuszewicz, Roman S.(1994) 'THE NATURE OF METAL-AZIDE INTERACTIONS IN A HIGH-VALENT TETRAAZIDO-MANGANESE(IV) COMPLEX. ISOLATION, STRUCTURE AND PROPERTIES, INCLUDING UV-*VIS*, EPR AND RESONANCE RAMAN SPECTROSCOPY OF [Mn(bpy)(N_3)$_4$] (bpy = 2,2'-bipyridine)', Journal of Coordination Chemistry, 33: 3, 257 — 269
To link to this Article: DOI: 10.1080/00958979408024284
URL: http://dx.doi.org/10.1080/00958979408024284

J. Coord. Chem., 1994, Vol 33, pp. 257–269
Reprints available directly from the publisher
Photocopying permitted by license only

THE NATURE OF METAL-AZIDE INTERACTIONS IN A HIGH-VALENT TETRAAZIDO-MANGANESE(IV) COMPLEX. ISOLATION, STRUCTURE AND PROPERTIES, INCLUDING UV-*VIS*, EPR AND RESONANCE RAMAN SPECTROSCOPY OF [Mn(bpy)(N_3)$_4$] (bpy = 2,2′-bipyridine)

BAKUL C. DAVE

Department of Chemistry and Biochemistry University of California at Los Angeles Los Angeles, CA 90024

and ROMAN S. CZERNUSZEWICZ*

Department of Chemistry, University of Houston, Houston, TX 77204

(Received on April 4, 1994)

A mononuclear high-valent tetraazidomanganese(IV) complex, [Mn(bpy)(N_3)$_4$] (bpy = 2,2′-bipyridine), which possesses two pairs of distinct metal-azide interactions, has been isolated from an *in situ* reaction between $[Mn_2O(O_2CCH_3)_2(bpy)_2(H_2O)_2]^{2+}$ [S. Menage, J.-J Girerd and A. Gleizes, *J. Chem. Commun.* 1988, 431] and sodium azide. The complex has been structurally characterized by single crystal X-ray crystallography and UV-*vis*, EPR and resonance Raman (RR) spectroscopic methods. The crystals are monoclinic, space group *C*2/c, with a = 16.570(3) Å, b = 13.946(3) Å, c = 7.019(1) Å, β = 111.17(3)°, and Z = 4. The two azides *trans* to the nitrogens of the bpy ligand show stronger Mn–N bonds compared to those *cis* to bpy. The difference in Mn-azide interactions is reflected in splittings of the ν(Mn–N_3) (373, 362 cm^{-1}), $\nu_s(N_3)$ (1354, 1335 cm^{-1}) and $\nu_{as}(N_3)$ (2055, 2038 cm^{-1}) stretching vibrational frequencies of the coordinated N_3^- as identified by RR spectroscopy. These modes are enhanced in resonance with the visible absorption band of [Mn(bpy)(N_3)$_4$] centered at 442 nm, indicating that the 442 nm electronic transition must have $N_3^- \rightarrow$ Mn(IV) charge-transfer character. A very rare example of a d^3 system with an isotropic g = 2 signal observed for the title complex indicates a nearly perfect octahedral ligand field around the Mn(IV) ion.

KEYWORDS: azide, tetraazidomanganese, Manganese (IV)

INTRODUCTION

Inorganic azides have long enjoyed industrial usefulness as detonators, generators of pure nitrogen gas in safety cushions (air bags), and photographic materials.[1] The

* Author for correspondence.

ability of the azide ions to act as detonators or as effective generators of nitrogen gas has been found to be a property of the polarization of the ordinarily symmetric azide anion brought about by complexation with a metal ion. Apart from its industrial usefulness, the azide ion, being very reactive, acts as an inhibitor in various biological systems by blocking the substrate binding sites.[1] In manganese biosystems, the azide ion is known to inihibit the superoxide dismutation in mononuclear superoxide dismutases *via* binding to the metal at the active site in both the Mn(II) and Mn(III) oxidation states.[2] The function of dinuclear active sites in Mn catalases, which catalyze the conversion of toxic peroxide to oxygen and water in certain bacteria, is also dramatically inhibited by azide.[3,4]

The metal-azide interaction is usually accompanied by intense ligand (azide) to metal charge-transfer electronic transition(s), which makes it an excellent probe to elucidate the structure and oxidation states of the active site by monitoring the resonance Raman (RR)[5] enhanced vibrations associated with the anion. In order to determine the nature of the metal-azide binding in Mn containing biomolecules, it is important to establish signature vibrations in well-defined inorganic model complexes.[6] Described in this work are the synthesis, structure and properties, including UV-*vis*, EPR and RR spectroscopy, of a high-valent Mn(IV) complex, $[Mn(bpy)(N_3)_4]$, possessing two crystallographically distinct metal-azide interactions.

MATERIALS AND METHODS

Synthesis

All chemicals and solvents (Aldrich, Milwaukee, WI) were of analytical grade and were used without further purification. The tetraazido-Mn(IV) complex, $[Mn(bpy)(N_3)_4]$, was isolated while trying to replace the water molecules in the (μ-oxo)bis(μ-carboxylato) Mn(III,III) dimer, $[Mn_2O(O_2CCH_3)_2(bpy)_2(H_2O)_2]^{2+}$,[7] with azide. Dimer formation was initiated by mixing 0.490 g (2 mmol) of $Mn(O_2CCH_3)_2 \cdot 4H_2O$ in methanol (20 mL) containing 3 mL of glacial acetic acid with 0.39 g (2.5 mmol) of bpy ligand to give a yellow colored solution. To this mixture was added 0.079 g (0.5 mmol) of $KMnO_4$ dissolved in 5 mL of water to give a red-brown solution containing $[Mn_2O(O_2CCH_3)_2(bpy)_2(H_2O)_2]^{2+}$.[7] This solution was then treated with 0.163 g (2.5 mmol) of NaN_3 dissolved in 5 mL water and left standing at 0°C. Black crystals of $[Mn(bpy)(N_3)_4]$ were afforded overnight which were purified by recrystallization in dichloromethane.

[Caution! The $[Mn(bpy)(N_3)_4]$ complex is potentially explosive, extremely shock sensitive and thermally unstable, and should be handled with appropriate care.]

Yield, 0.15 g (49% based on total Mn). *Anal.* Calcd. for $C_{10}H_8N_{14}Mn$(%): C, 31.64; H, 2.28; N, 51.68. Found: C, 30.18; H, 1.97; N, 54.71. Elemental analysis was performed at Texas Analytical Lab., Houston, Texas.

X-ray Structure Determination

A black needle of $[Mn(bpy)(N_3)_4]$ was mounted in a random orientation on a Siemens P4 automatic diffractometer operated at room temperature. The radiation used was Mo Kα monochromatized by a highly-ordered graphite crystal. The final

cell constants, as well as other pertinent information, are given in Table 1. Systematic absences led to two possible space group choices $C2/c$ or Cc. The statistics (0.940 found, 0.968 expected for $|E^2 - 1|$) clearly favored the centrosymmetric $C2/c$ and hence it was chosen for initial evaluation. The successful solution and refinement in this space group validated the choice. Intensities were measured using the θ–2θ scan technique to a maximum 2θ value of 45.0°, with the scan rate depending on the count obtained in rapid pre-scans of each reflection. Three standard reflections were monitored after every 100 data collected, and these showed no significant change. Stationary-background counts were recorded at the beginning and the end of scan, each for 0.5% of the total scan time. Of the 1219 reflections which were collected, 990 were unique (R_{int} = 0.0381). The linear absorption coefficient for Mo Kα radiation is 9.03 cm^{-1}. A semi-empirical absorption correction, based on azimuthal scans of several reflections, was applied, which resulted in transmission factors ranging from 0.7945 to 0.8615. The data were corrected for Lorentz and polarization effects.

The structure was solved using Siemens SHELXTL PLUS (PC version) direct methods program, which revealed the position of most of the non-hydrogen atoms in the molecule. The usual sequence of isotropic and anisotropic refinement using full-matrix least squares was followed, after which all hydrogens were entered in

Table 1 Crystallographic Data for [Mn(bpy)$(N_3)_4$].[a]

molecular formula	$C_{10}H_8N_{14}Mn$
formula wt	379.2
color and habit	black needles
crystal system	monoclinic
space group	$C2/c$
a, Å	16.570 (3)
b, Å	13.946 (3)
c, Å	7.019 (1)
β, deg	111.17 (3)
V, Å^3	1512.5
Z	4
crystal dimensions, mm	0.1 × 0.1 × 0.6
ρ(calc), g cm^{-3}	1.665
μ(Mo Kα), cm^{-1}	9.03
F(000)	764
T, K	298
2θ range, deg	3.5–45.0
scan range (total in ω), deg	1.2
scan speed range, deg min^{-1}	4–29.3
reflections collected	1219
independent reflections (R_{int} = 0.038)	990
reflections observed ($F > 4.0\sigma(F)$)	626
total variables	114
transmission coefficients	0.7945, 0.8615
R, R_w	0.059, 0.063
S(goodness-of-fit)	1.14

[a]Data collected on a Siemens P4 diffractometer operating in the θ–2θ scan mode (h, −1 to 17; k, −1 to 14; l, −7 to 17); graphite-monochromated Mo Kα X-radiation, λ = 0.71073 Å. Refinement was by a full-matrix least-squares method on F with a weighing scheme of the form $w^{-1} = [\sigma_c^2(F_o) + 0.0008|F_o|^2]$, where $\sigma_c^2(F_o)$ is the variance in F_o due to counting statistics. The maximum and minimum peaks on the final difference Fourier map corresponded to 0.37 and −0.39 e Å^{-3}. [b]$R = \Sigma(||F| - |F_c||)/\Sigma(|F_o|)$, $R_w = [\Sigma w(|F_o| - |F_c|)^2/\Sigma w(|F_o|)^2]^{1/2}$.

their idealized positions (d(C–H) = 0.96 Å) and constrained to riding motion, with a single isotropic temperature factor (U_{iso} = 80 × 10^{-3} Å^2) for each. The final cycle of full-matrix least-squares refinement was based on 626 observed reflections ($F > 4.0\sigma(F)$) and 114 variable parameters and converged with weighted and unweighted agreement factors of R = 0.0594 and R_w = 0.0638. The final atomic coordinates and equivalent isotropic displacement parameters for the non-hydrogen atoms are given in Table 2, important distances and bond angles are listed in Table 3, and an ORTEP diagram of [Mn(bpy)$(N_3)_4$] is given in Figure 1.

Physical Measurements

Resonance Raman spectra of [Mn(bpy)$(N_3)_4$] and its $^{15}N^{14}N_2$ isotropically labeled analog were obtained in CH_2Cl_2 solution (~1 mM) at room temperature by excitation with a 457.9 nm laser line (~50 mW laser power) from a Coherent 90–6 Ar^+ ion laser. The ^{15}N-labeled compound for RR measurements was prepared as described above by reducing ten times the amounts of all reagents and using sodium azide-containing $^{15}N^{14}N_2$ anion, which was obtained from Cambridge Isotope Laboratories (Andover, MA). The scattered photons were collected *via* backscattering geometry fromr a spinning NMR tube.[8] A scanning Raman instrument equipped with a Spex 1403 double monochromator and a Hamamatsu 928 photomultiplier detector system was used to record the spectra under the control of a Spex DM3000 microcomputer system, as described in detail elsewhere.[6] Due to the photolability of [Mn(bpy)$(N_3)_4$], the spectra were recorded over small frequency ranges (100–300 cm^{-1}) and fresh solution samples were employed for each individual scan. An average of multiple scans (6–8) were taken to improve the signal to noise ratio. Raman data manipulation was performed using LabCalc software (Galactic Industries Inc.) on a 486-DX 33 MHz PC microcomputer. Baseline correction and data smoothing were performed utilizing the two-point baseline correction and fast-Fourier transform smoothing LabCalc routines. A smoothing factor of 0.1 was used consistently as it removed high-frequency noise without distortion to band shape or height. A Hewlett-Packard 8-pen ColorPro graphics plotter was used to hardcopy output of spectra.

Table 2 Atomic Coordinates (× 10^4) and Equivalent Isotropic Displacement Parameters (Å × 10^3) for Non-Hydrogen Atoms in [Mn(bpy)$(N_3)_4$].

Atom	x	y	z	$U(eq)^a$
Mn	0	7455 (2)	2500	26 (1)
N(1)	-832 (4)	6295 (5)	2093 (11)	25 (3)
N(2)	-217 (5)	7402 (6)	-441 (10)	38 (3)
N(3)	-910 (5)	7648 (7)	-1629 (13)	46 (4)
N(4)	-1579 (7)	7846 (8)	-2835 (15)	79 (5)
N(5)	-920 (5)	8360 (5)	2033 (14)	42 (4)
N(6)	-891 (5)	8955 (7)	3331 (15)	45 (4)
N(7)	-915 (7)	9510 (9)	4442 (19)	103 (7)
C(1)	-473 (5)	5433 (6)	2193 (12)	27 (3)
C(2)	-981 (6)	4607 (7)	1718 (13)	33 (4)
C(3)	-1868 (6)	4687 (7)	1145 (14)	39 (4)
C(4)	-2220 (6)	5572 (8)	1113 (14)	44 (4)
C(5)	1696 (5)	6375 (7)	1590 (14)	34 (4)

[a]Equivalent isotropic U defined as one-third of the trace of the orthogonalized U_{ij} tensor.

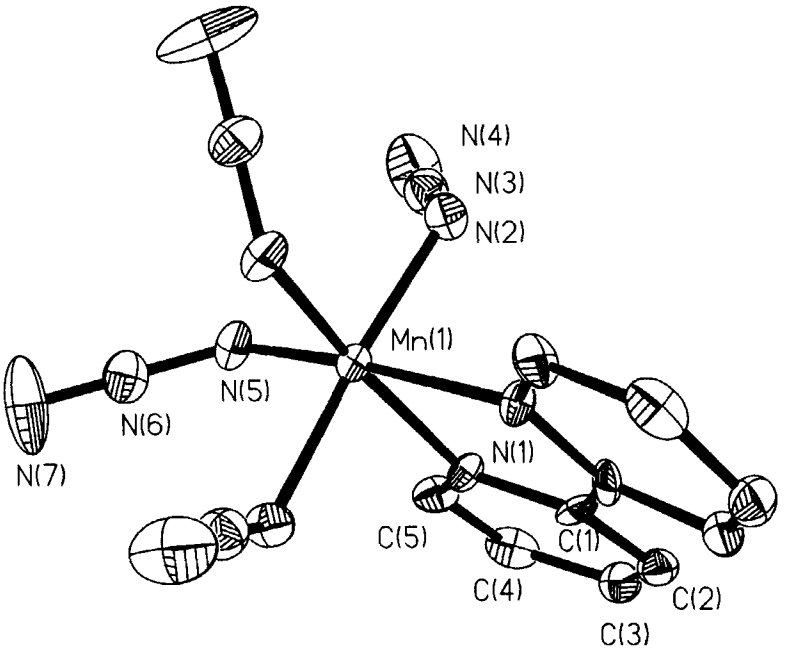

Figure 1 ORTEP view of $[Mn(bpy)(N_3)_4]$ with the atom labeling scheme (40% probability ellipsoids; hydrogen atoms omitted). Selected bond lengths and bond angles are listed in Table 3.

Absorption spectra were obtained on a HP-8542 diode array spectrophotometer in 1 mm quartz cuvettes using approximately 1 mM solutions with CH_2Cl_2 as a solvent. Magnetic moments were obtained by using a Johnson-Matthey MSB-1 magnetic susceptibility balance. The solid state EPR spectrum of $[Mn(bpy)(N_3)_4]$ was recorded on a Bruker ER200 E-SRC spectrometer equipped with a liquid-nitrogen dewar and a Varian variable-temperature controller. DPPH (g = 2.0037) was used as an external standard. Cyclic voltammetric measurements were carried out on an IBM Model 225 voltammetric analyzer by utilizing a three-electrode electrochemical cell. The working electrode was platinum, and the potential reference was a saturated calomel electrode (SCE).

RESULTS AND DISCUSSION

Synthesis

The isolation of $[Mn(bpy)(N_3)_4)$ from the *in situ* reaction of azide with the $[Mn_2(\mu\text{-}O)(\mu\text{-}O_2CCH_3)_2]^{2+}$ core demonstrate the fragile nature of this core in the presence of a strong ligand like azide. Similar lability of this core was also observed for the analogous complexes with tridentate ligands tacn and Me_3tacn.[9] However,

breaking the oxo-bridged core in $[Mn_2O(O_2CCH_3]_2(tacn)_2]^{2+}$ leads to isolation of the Mn(III) species, $[Mn(tacn)(N_3)_3]$,[9a] as opposed to the Mn(IV) species obtained with the bidentate ligand bpy. This destruction of the dinuclear μ-oxo core supported by two acetato bridges is particularly noteworthy in light of the fact that in the structurally analogous dichloro complex, $[Mn_2O(O_2CPh)_2(bpy)_2(Cl)_2]$, the chloride ions can be replaced with azide by using NaN_3 to give $[Mn_2O(O_2CPh)_2(bpy)_2(N_3)_2]$.[10] The $[Mn(bpy)(N_3)_4]$ complex is stable at room temperature in direct contrast to the tetrachloro analog, $[Mn(bpy)Cl_4]$, which decomposes at room temperature.[11] The stronger π-acceptor ability of azide ion might be an important factor in formation and stabilization of $[Mn(bpy)(N_3)_4]$.

Crystal and Molecular Structure

The high-valent $[Mn(bpy)(N_3)_4]$ complex crystallizes in the monoclinic space group $C2/c$ with cell constants $a = 16.570(3)$, $b = 13.946(3)$ and $c = 7.019(1)$ Å, $\beta = 111.17(3)°$, $V = 1512.5(3)$ Å^3, and four molecules per unit cell. Figure 1 shows the molecular structure of $[Mn(bpy)(N_3)_4]$ and the atom-labeling scheme, while Table 3 lists important bond distances and angles. The structure of $[Mn(bpy)(N_3)_4]$ has a crystallographically imposed C_2 axis of symmetry with two equivalent pairs of terminally bound azides and two nitrogens from bpy completing a distorted octahedral arrangement around the metal center. The two azides *trans* to the bpy nitrogens show stronger Mn–N bonds (1.914(8) Å) as compared to the azides *cis* to bpy (1.965(7) Å).

Electronic Absorption Spectrum

The UV-vis spectrum of $[Mn(bpy)(N_3)_4]$ in dichloromethane, shown in Figure 2, exhibits three intense absorptions at 442 (22,000), 290 (33,000) and 244 nm (36,000 $M^{-1}cm^{-1}$). For a coordinated azide ion, the Mn-N_3 group vibrations are expected to be coupled with the charge transfer (CT) electronic transitions from azide to the metal atom, and the band at 442 nm is assigned to the $N_3^- \rightarrow$ Mn(IV) CT transition on the basis of strong enhancements of the Mn–azide and intraazide stretching modes observed in the RR spectrum by excitation with a 457.9-nm laser line (*vide infra*). From N_3^- several CT transitions can take place to the acceptor

Table 3 Selected Bond Lengths (Å) and Bond Angles (deg) for $[Mn(bpy)(N_3)_4]$.

Bond Lengths					
Mn(1)-N(1)	2.077 (7)	Mn(1)-N(2)	1.965 (7)	Mn(1)-N(5)	1.914 (8)
N(2)-N(3)	1.200 (10)	N(3)-N(4)	1.160 (11)	N(5)-N(6)	1.220 (13)
N(6)-N(7)	1.109				
Bond Angles					
N(1)-Mn(1)-N(2)	88.0 (3)		N(1)-Mn(1)-N(5)	92.4 (3)	
N(2)-Mn(1)-N(5)	90.7 (4)		N(1)-Mn(1)-N(1A)	77.7 (4)	
N(2)-Mn(1)-N(1A)	88.6 (3)		N(5)-Mn(1)-N(1A)	170.1 (3)	
N(2)-Mn(1)-N(2A)	175.7 (5)		N(5)-Mn(1)-N(2A)	92.1 (4)	
N(5)-Mn(1)-N(5A)	97.5 (5)		Mn(1)-N(2)-N(3)	119.1 (8)	
Mn(1)-N(5)-N(6)	120.5 (6)		N(2)-N(3)-N(4)	176.6 (11)	
N(5)-N(6)-N(7)	175.8 (9)				

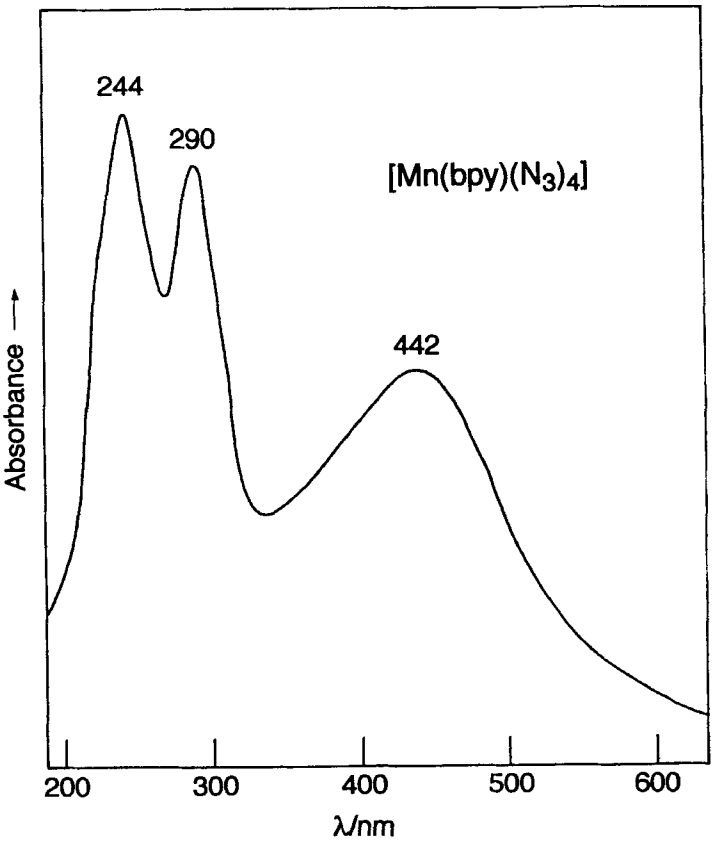

Figure 2 Electronic absorption spectrum of $[Mn(bpy)(N_3)_4]$ in CH_2Cl_2.

d-orbitals on the metal, which are divided into two groups, d_π and d_σ, with an energy separation Δ. The difference of 152 nm (~12 000 cm^{-1}) between the maxima of the two lowest energy bands in $[Mn(bpy)(N_3)_4]$ is comparable to the Δ value for Mn(IV) (~20 000 cm^{-1}) complexes.[12] The bands at 442 and 290 nm could therefore be assigned as $N_3^- \rightarrow Mn(d_\pi)$ and $N_3^- \rightarrow Mn(d_\sigma)$ CT transitions, respectively, with the transitions probably originating from different orbitals on the azide.

Previously, CT transitions near 459 nm were assigned as metal to ligand in porphyrinic $(N_3)Mn(III)TMP$.[13] In light of the very high oxidation state of manganese atoms in $[Mn(bpy)(N_3)_4]$, the possibility of these transitions being metal to ligand CT seems unlikely. The Mn(III) oxidation state with a highly donating porphyrin macrocycle in $(N_3)MnTMP$ is sufficiently electron rich to donate electron density to N_3^- in the excited state. Moreover, while the Mn(III) oxidation state can undergo an oxidative CT transition, the Mn(IV) state is highly preferential towards a reductive transition and, therefore, the direction of charge transfer in $[Mn(bpy)(N_3)_4]$ is expected to be ligand (N_3^-) to metal (Mn(IV)).

Resonance Raman Spectra

The RR spectra of [Mn(bpy)$(N_3)_4$) obtained at room temperature in CH_2Cl_2 solutions with 457.9-nm excitation are informative and show strong resonance enhancement of the modes associated with the Mn(IV)-N_3 units, as established by their frequency shifts registered upon substitution with terminally-labeled sodium azide, $Na^{15}NN_2$. The results are presented in Figure 3. In the low frequency region there are two RR bands at 362 and 373 cm^{-1} for the natural abundance sample which shift to 359 and 370 cm^{-1}, respectively, on isotopic labeling. The vibrations associated with stretching of the Mn–N_{azide} bonds, ν(Mn–N_3), are expected to occur in this region. The fact that two bands are observed in the RR spectrum with identical isotope shifts implies the presence of two distinctive Mn-N_{azide} interactions. These vibrational results are consistent with the differences in metal-azide bond strengths observed in the X-ray crystal structure of the complex which shows two pairs of distinct Mn–N_{azide} bond lengths (Table 3). Thus, the higher frequency peak at 373 cm^{-1} could be assigned to the Mn–N_{azide} oscillator *trans* to the bpy nitrogens, whereas the lower frequency vibration at 362 cm^{-1} is ascribed to the longer Mn–N_{azide} interaction *cis* to bpy ligand. By using Badger's rule $K \propto (r_e - 0.68)^{-3}$, where r_e is the equilibrium bond length and K is the stretching force constant],[14] the frequency difference of 11 cm^{-1} observed between the two –N_3) peaks is consistent with the Mn–N_{azide} bond length variation (~0.050 Å) observed in the crystal structure (Table 3).

With the porphyrinic ligand TMP, the ν(Mn–N_3) vibration was found to occur at 349 cm^{-1} in the infrared spectrum of N_3Mn(III)TMP.[13] Higher frequencies of the ν(Mn–N_3) stretches observed in [Mn(bpy)$(N_3)_4$] are consistent with the higher charge on the Mn atom. Also, due to the strongly electron donating nature of the porphyrin macrocycle, the interaction of the metal with the azide anion in N_3Mn(III)TMP is expected to be diminished to a certain extent, lowering the bond strength and the frequency of vibration. Thus, the 362 and 373 cm^{-1} RR frequencies can be ascribed to stretching motions of the Mn–N_{azide} bonds with a considerable degree of confidence. In addition, whereas the ν(Mn–N_3) stretching modes are significantly enhanced in [Mn(bpy)$(N_3)_4$], the analogous vibration in the porphyrinic complex N_3Mn(III)TMP is not enhanced, implying that the M–N_{azide} bond length in the latter compound does not change much as a result of the charge transfer. If the nature of charge transfer is azide(π) to porphyrin(π^*) or alternatively M(d_π) to azide(π^*) as has been suggested,[13] then there would be minimal resultant displacement along the ν(Mn–N_3) coordinate during the transition, thereby showing little or no enhancement of this mode. It is clear that the direction of charge transfer transition near 450 nm in the two complexes must be opposite.

Figure 3 also reveals two pairs of $^{15}NN_2$ isotope sensitive bands centered near 1340 and 2050 cm^{-1} where, respectively, the symmetric (in-phase) and asymmetric (out-of-phase) intraazide nitrogen-nitrogen streching vibrations are known to occur. Again, the appearance of doublets in each spectral region signifies two different metal-azide interactions in [Mn(bpy)$(N_3)_4$], in agreement with crystallographic data (Table 3). The asymmetric stretch, $\nu_{as}(N_3)$, is not Raman active in the centrosymmetric non-ligated azide anion ($D_{\infty h}$ symmetry). Coordination to a metal, however, polarizes the azide moiety and destroys the center of inversion, making it asymmetric in the ground electronic state. This explains the observation of both the $\nu_s(N_3)$ and $\nu_{as}(N_3)$ intraazide stretches in the RR spectrum, as both become

Raman-active upon coordination of N_3^- to Mn(IV). In addition, the $N_3^- \rightarrow$ Mn(IV) CT excited state of the bound azide unit would then be more symmetric, *via* an asymmetric displacement of the three nitrogen atoms. Taken together, the preceding arguments imply that the CT transition from N_3^- to Mn(IV) results in changes in bond lengths in the N–N–N unit that mimic the $\nu_{as}(N_3)$ vibrational mode. Indeed, the RR spectrum of $[Mn(bpy)(N_3)_4]$ shows two azide dependent peaks at 2038 and

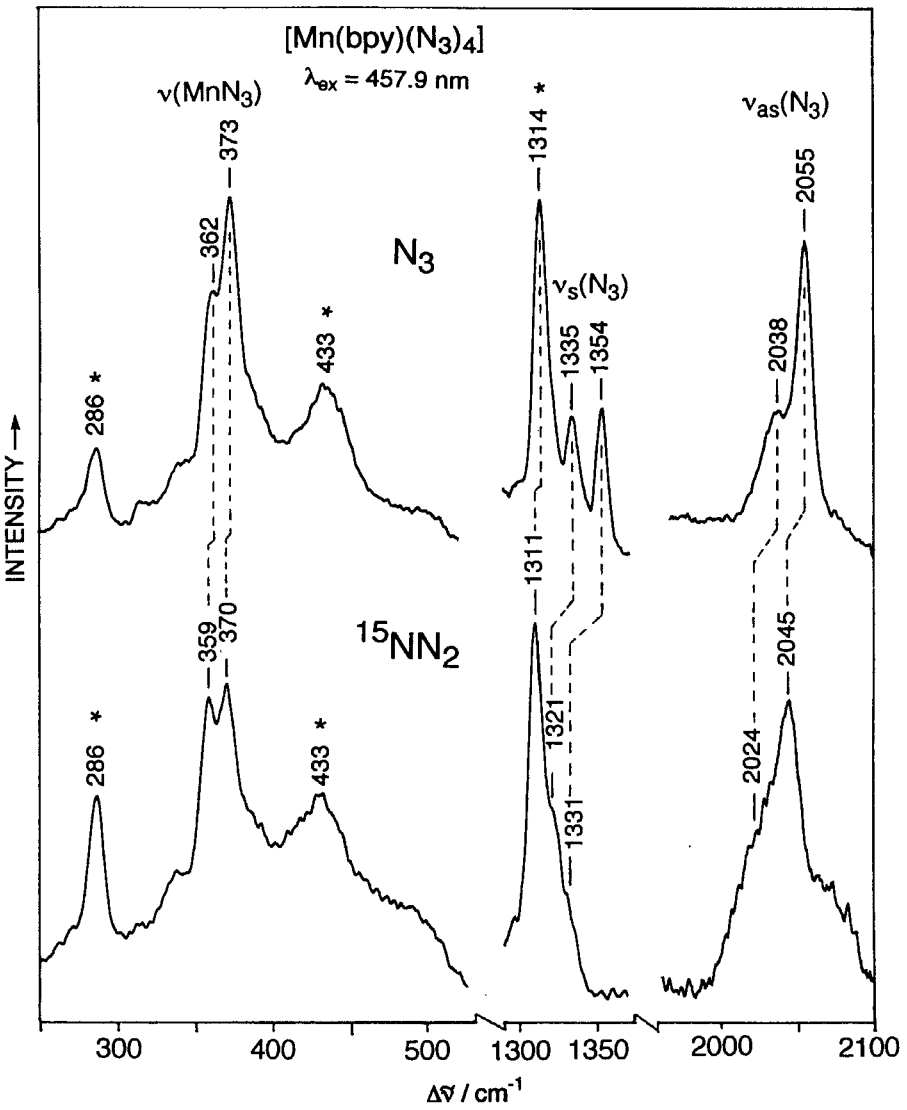

Figure 3 Room temperature RR spectra of $[Mn(bpy)(N_3)_4]$ and its $^{15}N^{14}N_2$ labeled isotopomer in CH_2Cl_2 solution excited at 457.9 nm; 50-mW laser power, 6-cm^{-1} slit widths. The bands marked by asterisks are due to bpy vibrations.

2055 cm^{-1}, which downshift to 2024 and 2045 cm^{-1} on $^{15}N^{14}N_2$ labeling. A similar $\nu_{as}(N_3)$ peak in the (N_3)MnTMP RR spectrum was found to occur at ~2040 cm^{-1}, the lower frequency consistent with the more symmetric axial azide ligand in this complex.[13] Enhancement of the $[Mn(bpy)(N_3)_4]$ $\nu_{as}(N_3)$ modes by 457.9-nm excitation wavelength also strongly supports the assignment of the visible absorption band of $[Mn(bpy)(N_3)_4]$ at 442 nm as the azide to metal CT transition.

Magnetism and EPR Spectrum

The room temperature magnetic moment of 3.94 μ_B corresponds well to the theoretically predicted spin only value (3.87 μ_B) for three unpaired electrons of d^3 Mn(IV) species. For a d^3 system two EPR resonances centered at $g \approx 4$ (strong) and $g \approx 2$ (weak) are typically observed.[15-17] The EPR signal of $[Mn(bpy)(N_3)_4]$, which is presented in Figure 4, is particularly interesting in that it shows only a very strong $g \approx 2$ signal at liquid nitrogen temperature. This difference can be explained as follows.

For Mn(IV) complexes, a d^3 system, in a crystal field of strict octahedral symmetry, a $^4A_{2g}$ ground state is expected. Spin-orbit coupling or a low-symmetry ligand field may mix this ground state with excited states (configuration interaction) and split the quartet ground state into two Kramer's doublets separated by $2(D^2 + 3E^2)^{1/2}$, where D and E are the axial and rhombic zero-field splitting constants, respectively, such that $D/E \geq 3$.[15]

In the limiting approximation with $D >> E$, the zero-field splitting is simply $2D$. The EPR spectra of d^3 systems are expected to be highly dependent on the value of D as compared to the resonance quantum energy $h\nu$(= 0.317 cm^{-1} for X-band).[15] In the case of $2D >> h\nu$ (large distortion), the EPR signal consists of two

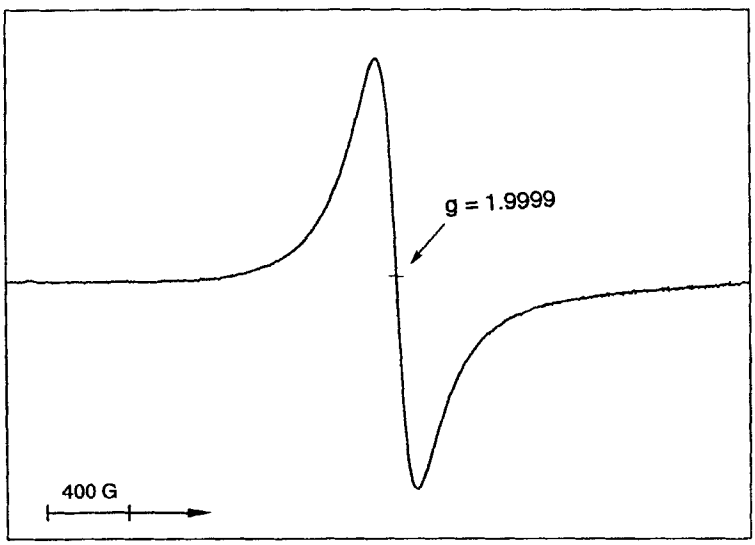

Figure 4 EPR spectraum of a solid sample of $[Mn(bpy)(N_3)_4]$ at 77 K, showing the $g = 2$ transition. Microwave frequency 9.18 GHz; field modulation amplitude, 32 G; time constant, 0.5; receiver gain, 2.

resonances at $g \approx 2$ and $g \approx 4$ with the latter being much more intense. As the value of D decreases with respect to hν, the $g \approx 4$ resonance diminishes in intensity whereas the $g \approx 2$ signal gains intensity, and, in the case of $2D << h\nu$ (small distortion), the dominant signal is expected to be the one at $g \approx 2$. A large number of instances have been reported where the observed EPR signal can be classified between the realms of these two simplified cases;[15-19] examples of the $2D << h\nu$ situation for Mn(IV) are sparse however.[18,17b]

The low C_2 symmetry of the $[Mn(bpy)(N_3)_4]$ complex, with a formally rhombic coordination environment as observed in the crystal structure, and the fact that two different ligands with highly disparate ligand field strengths coordinate the central metal ion, would predict a rhombic or axially distorted EPR signal with resonances at $g \approx 2$ and 4. In sharp contrast to the expectation, the observed EPR signal of $[Mn(bpy)(N_3)_4]$ at 77 K consists only of a strong isotropic resonance centered at $g = 1.999$ that is devoid of any hyperfine interactions (Fig. 4). As such the X-band EPR spectrum of $[Mn(bpy)(N_3)_4]$ not only conforms to the rare Mn(IV) $2D << h\nu$ case but reveals an effective electronic environment around the metal atom that is a nearly perfect octahedron (*i.e.*, $D \approx 0$). A $g \approx 2$ isotropic signal has previously been documented in K_2MnCl_6, where an octahedral environment has been structurally verified,[19] and now in $[Mn(bpy)(N_3)_4]$. In the case of *trans*-$[Cr(py)_4(OH)_2]^+$ and *trans*-$[Cr(NH_3)_4(OH)_2]^+$ complexes, which display essentially isotropic $g \approx 2$ EPR signals with minor components near $g \approx 4$, the magnitude of D has been calculated to be less than 0.01 cm^{-1}.[15b] Also in the two Schiff-base N_4O_2 coordinated complexes, a very small D value (~0.012 cm^{-1}) was recently calculated, even though the $Mn(IV)N_4O_2$ coordination spheres were structurally determined to be rhombically distorted.[18c] It is also interesting to note that $[Mn(HB(3,5\text{-}Me_2pz)_3)_2]^{2+}$ with a nearly octahedral $Mn(IV)N_6$ environment shows a strongly axially distorted EPR signal[16d] whereas the neutral $[Mn(bpy)(N_3)_4]$ with a rhombically distorted structure shows a signal indicating minimal ligand field distortion of the electronic environment with a $^4A_{2g}$ ground state.

Electrochemistry

The cyclic voltammetry of $[Mn(bpy)(N_3)_4]$ shows a reversible wave at + 0.48 V (*vs* SCE) corresponding to the Mn(IV)/Mn(III) reduction and an irreversible wave at $E_{1/2} = -0.16$ V (Fig. 5). The positive potential implies a spontaneous reduction towards the Mn(III) oxidation state. The Mn(IV)/Mn(III) reduction is reversible with a peak-to-peak separation (ΔEp) of 0.12 V. The compound did not show any oxidative electrochemistry as expected for the Mn(IV) complex. With the all pyrazolyl N_6-donor ligation in the complex $[Mn(HB(3,5\text{-}Me_2pz)_3)_2]$, the Mn(IV)/Mn(III) reduction was found to occur at 1.35 V (*vs* SCE).[16d] The lower reduction potential for $[Mn(bpy)(N_3)_4]$ is an indicator of the stabilization of the Mn(IV) oxidation state afforded by the azide ligands due to the greater extent of metal to ligand back-bonding.

CONCLUSIONS

A monomeric high-valent Mn(IV) complex with $N_2N'_4$ coordination, which exhibits a comparatively rare set of physical and chemical properties, has been

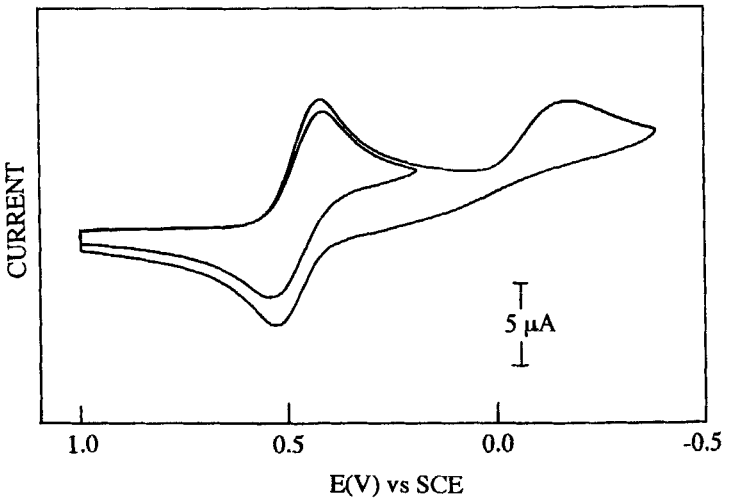

Figure 5 Cyclic voltammograms of $[Mn(bpy)(N_3)_4]$ in CH_2Cl_2, 0.1 M TBAP at a scan rate of 0.1 V/s.

isolated and structurally and spectroscopically characterized. The intense $N_3^- \rightarrow Mn(IV)$ CT transition at 442 nm ascertains the viability of the azide anion as a potential vibrational probe and leads to enhancement of the Mn-azide and intraazide stretching vibrations in RR spectra. The observed $\nu(Mn\text{–}N_3)$, $\nu_s(N_3)$ and $\nu_{as}(N_3)$ RR frequencies serve as useful signatures of high-valent Mn-azide interactions and should be beneficial in characterization of similar interaction(s) in manganobiomolecules. The low reduction potential obtained for this complex, as compared to the all pyrazolyl N_6 coordination, indicates a stabilization of the Mn(IV) oxidation state by azide ligands. Combination of bpy and azide nitrogens in $[Mn(bpy)(N_3)_4]$ provides an effective ligand field around the Mn(IV) ion that is a nearly perfect octahedron, and $[Mn(bpy)(N_3)_4]$ serves as a very rare example of a d^3 system with an isotropic $g = 2$ signal. This complex can, in principle, liberate four moles of N_2 gas per mole, and therefore could be useful in applications requiring an impact-sensitive N_2 gas generator. Finally, the presence of two different sets of azide coordination makes this complex potentially suitable for shock-trains with the polarized azides acting as initiators and the more symmetrical azides as propagators of the train, and $[Mn(bpy)(N_3)_4]$ may find use as an energetic material.

Acknowledgements

This work was supported by a grant GM-48370 from the National Institutes of General Medical Sciences, NIH. B. C. D. thanks the Robert A. Welch Foundation for a graduate student fellowship. We are grateful to Dr. Carl J. Carrano (Southwest Texas State University) for his assistance in both solving the X-ray crystal structure and recording the low temperature EPR spectra of $[Mn(bpy)(N_3)_4]$. Miss Tina Smeal is thanked for assistance in the X-ray data collection and refinement.

References

1. H.D. Fair and R.F. Walker (eds), *Energetic Materials* (Plenum Press, New York, 1977), Vol. 1–2.
2. J.W. Whittaker and M.M. Whittaker, *J. Am. Chem. Soc.* **113**, 5528 (1991).
3. (a) Y. Kono and I. Fridovich, *J. Bacteriol.* **155**, 742 (1983). (b) Y. Kono and I. Fridovich, *J. Biol. Chem.* **258**, 6015 (1983). (c) W.F. Beyer, Jr. and I. Fridovich, *Biochemistry* **24**, 6460 (1985). (d) R.M. Fronko, J.E. Penner-Hahn, and C.J. Bender, *J. Am. Chem. Soc.* **110**, 7554 (1988). (e) G.S. Waldo, R.M. Fronko, and J.E. Penner-Hahn, *Biochemistry* **30**, 10486 (1991). (f) G.S. Waldo, S. Yu, and J.E. Penner-Hahn, *J. Am. Chem. Soc.* **114**, 5869 (1992). (g) J.E. Penner-Hahn, in *Manganese Redox Enzymes*, V.L. Pecoraro, Ed. (VCH Publishers, New York, 1992) pp 29–46.
4. (a) V.V. Barynin and A.I. Grebenko, *Dokl. Akad. Nauk. SSSR* **286**, 461 (1986). (b) V.V. Barynin, A.A. Vagin, V.R. Melik-Adamyan, A.I. Grebenko, S.V. Khangulov, A.N. Popov, M.E. Andrianova, and B.K. Vainshtein, *Dokl. Akad. Nauk. SSSR* **288**, 877 (1986). (c) S.V. Khangulov, V.V. Barynin, and S.V. Antonyuk-Barynina, *Biochim. Biophys. Acta.* **102**, 25 (1990).
5. Abbreviations used: bpy, 2,2′-bipyridine; tacn, 1,4,7-triazacyclononane; Me_3tacn, *N,N′,N″*-trimethyl-1,4,7-triazacyclononane; $HB(3,5\text{-}Me_2pz)_3^-$, hydrotris(1-(3,5-dimethyl)pyrazolyl)borate; TMP, tetramesitylporphyrin; RR, resonance Raman; CT, charge transfer; EPR, electron paramagnetic resonance; SCE, saturated calomel electrode.
6. R.S. Czernuszewicz, in *Methods in Molecular Biology*, C. Jones, B. Mulloy, and A.H. Thomas, eds. (Humana Press, Totowa, NJ, 1993), Vol. 17, pp 345–374.
7. S. Menage, J.-J. Girerd, and A. Gleizes, *J. Chem. Soc. Chem. Commun.* **1988**, 431.
8. R.S. Czernuszewicz, *Appl. Spectrosc.* **40**, 571 (1986).
9. (a) K. Wieghardt, U. Bossek, B. Nuber, and J. Weiss, *Inorg. Chim. Acta.* **126**, 39 (1987). (b) K. Wieghartdt, U. Bossek, B. Nuber, J. Weiss, J. Bonovoisin, M. Corbella, S.E. Vitols, and J.-J. Girerd, *J. Am. Chem. Soc.* **110**, 7398 (1988).
10. J.B. Vincent, K. Folting, J.C. Huffmann, and G. Christou, *Biochem. Soc. Trans.* **16**, 822 (1988).
11. H.A. Goodwin and R.N. Sylva, *Aust. J. Chem.* **18**, 1743 (1965).
12. C.K. Jørgensen, *Absorption Spectra and Chemical Bonding in Complexes* (Pergamon, New York, 1962), 3rd ed., p. 110.
13. R.S. Czernuszewicz, W.-F. Wagner, G.B. Ray, and K. Nakamoto, *J. Mol. Struct.* **242**, 99 (1991).
14. (a) R.M. Badger, *J. Chem. Phys.* **3**, 710 (1935). (b) D.R. Herschbach and V.W. Laurie, *J. Chem. Phys.* **35**, 458 (1961).
15. (a) J.C. Hampel, L.O. Morgan, and W.B. Lewis, *Inorg. Chem.* **9**, 2064 (1970). (b) E. Pedersen and H. Toftlund, *Inorg. Chem.* **13**, 1603 (1974).
16. (a) M.J. Camenzind, F.J. Hollander, and C.L. Hill, *Inorg. Chem.* **22**, 3776 (1983). (b) J.R. Hartman, B.M. Foxman, and S.R. Cooper, *Inorg. Chem.* **23**, 1381 (1984). (c) M.W. Lynch, D.N. Hendrickson, B.J. Fitzgerald, and C.G. Pierpont, *J. Am. Chem. Soc.* **106**, 2041 (1984). (d) M.K. Chan and W.H. Armstrong, *Inorg. Chem.* **28**, 3777 (1989). (e) S.K. Chandra, P. Basu, D. Ray, S. Pal, and A. Chakravorty, *Inorg. Chem.* **29**, 2423 (1990). (f) S. Dutta, P. Basu, and A. Chakravorty, *Inorg. Chem.* **30**, 4031 (1991). (g) S.M. Saadeh, M.S. Lah, and V.L. Pecoraro, *Inorg. Chem.* **30**, 8 (1991).
17. (a) J.T. Groves, and M.K. Stern, *J. Am. Chem.* Soc. **109**, 3812 (1987). (b) M. Shappacher, and R. Weiss, *Inorg. Chem.* **26**, 1190 (1987). (c) R.S. Czernuszewicz, Y.O. Su, M.K. Stern, K.A. Macor, D. Kim, J.T. Groves, and T.G. Spiro, *J. Am. Chem. Soc.* **110**, 4158 (1988).
18. (a) K.L. Brown, R.M. Golding, P.C. Healy, K.J. Jessop, and W.C. Tennant, *Aust. J. Chem.* **27**, 2075 (1974). (b) S. Pal, P. Ghosh, and A. Chakravorty, *Inorg. Chem.* **24**, 3704 (1985). (c) S. Chandra and A. Chakravorty, *Inorg. Chem.* **31**, 760 (1992).
19. D.T. Richens and D.T. Sawyer, *J. Am. Chem. Soc.* **101**, 3681 (1979).